J Appl Electrochem (2009) 39:213–225
DOI 10.1007/s10800-008-9657-5

ORIGINAL PAPER

A method for rough estimation of the catalyst surface area in a fuel cell

Tanja Vidaković · Mihai Christov · Kai Sundmacher

Received: 27 March 2008 / Accepted: 21 August 2008 / Published online: 6 September 2008

Abstract A method for a rough estimation of the catalyst surface area in a fuel cell is developed. It is based on the deconvolution of experimental CO oxidation data by use of a mathematical model. The kinetic parameters of the model are determined by fitting the experimental curves. The experimental data are collected at different sweep rates (2–100 mV s^{-1}) and at different temperatures (room −60.0 °C). The model can predict the sweep rate dependence of the CO oxidation onset potential, the peak current, the peak potential and the peak broadness. The model is further used for the prediction of the baseline in the presence of CO and for calculation of the CO charge consumed up to half peak potential. It is obtained that the latter value is constant at different sweep rates and that the baseline deviates from linearity already at low sweep rates (2 mV s^{-1}), but not very significantly (2.0% in comparison to 8.8% at 100 mV s^{-1}, based on calculated CO charge). It is suggested that lower sweep rates should be used for experimental surface area determination.

Keywords Fuel cell · PtRu catalyst · Surface area · Mathematical model · Peak deconvolution

T. Vidaković (✉) · K. Sundmacher
Process Systems Engineering, Otto-von-Guericke-University Magdeburg, Universitätsplatz 2, 39106 Magdeburg, Germany
e-mail: vidakovi@mpi-magdeburg.mpg.de

M. Christov
Department of Physical Chemistry, University of Chemical Technology and Metallurgy, 1756 Sofia, Bulgaria

K. Sundmacher
Max-Planck-Institute for Dynamics of Complex Technical Systems, Sandtorstr. 1, 39106 Magdeburg, Germany

Nomenclature

$B_{2\theta}$	Width of the X-ray diffraction peak at half height/rad
$B^{r}_{2\theta}$	Width of the X-ray diffraction peak at half height for a standard compound/rad
c_{DL_Me}	Double layer capacitance of metal surface/mF
d	Average particle size/nm
e	Elementary charge/C (1.9×10^{-19} C)
E	Potential/V
$E_{a,i}$	Activation energy for the surface reaction/ kJ mol^{-1}
E_{ini}	CO adsorption potential/V
F	Faraday constant/C mol^{-1} (96,485 C mol^{-1})
c_f	Constant (Eq. 16)/–
g_i	Heterogeneity/interaction factor of the ith step/–
ΔH_{ads}	Enthalpy of adsorption of step 1/kJ mol^{-1}
I	Current/A
k_i	Reaction constant for the ith step/s^{-1}
N_A	Avogadro constant (6.022×10^{23} mol^{-1})
n_e	Number of exchanged electrons/–
N_{max}	Maximal number of the reaction sites on the surface/–
Q_{CO}	CO charge calculated by use of a model/C
Q_m	Charge for formation of a monolayer of monovalent adsorbed species/C
r_i	Reaction rate for the ith step/s^{-1}
R	Universal gas constant/J mol^{-1} K^{-1} (8.314 J mol^{-1} K^{-1})
S	CO surface area/cm^2
S_{XRD}	Specific surface area/m^2 g^{-1}
t	Time/s
T	Temperature/K
wt	Weight fraction/–
x_i	Atomic fraction of Pt or Ru atoms on the surface/–
α_i	Charge transfer coefficient for the ith step/–

β_i	Symmetry factor for the ith step/–
ε_{CO}	Model predicted CO charge up to half peak potential/–
ε_{rel}	Relative CO charge error/–
θ_i	Surface coverage of different species on the surface/–
θ_{max}	Angle at the X-ray diffraction peak maximum/rad
λ	Wavelength of X-ray/nm (here 0.1541874 nm)
v	Sweep rate/V s^{-1}
ρ	Density/g cm^{-3}
χ	Molar fraction/–

Subscripts

1	OH adsorption reaction
−1	OH desorption reaction
CO	Refers to CO adsorbed on the surface
OH	Refers to OH adsorbed on the surface
2_Pt	Surface reaction on platinum (step 2)
2_Ru	Surface reaction on ruthenium (step 2)
CO_Pt	CO adsorbed on platinum
CO_Ru	CO adsorbed on ruthenium
DL	Double layer
$I = I_{p/2}$	Half peak potential
Pt	Platinum
PtRu	Platinum ruthenium alloy
Ru	Ruthenium

1 Introduction

The CO oxidation on the surface of noble metal catalysts (platinum or platinum ruthenium) is a well studied reaction due to its relative simplicity and its use as a model reaction in both experimental and theoretical studies [1, 2]. It has also a great relevance in applied studies, since CO acts as a poison in a Polymer Electrolyte Membrane (PEM) fuel cell [3, 4], and is an intermediate generated during methanol oxidation in the Direct Methanol Fuel Cell (DMFC) [5].

During the oxidation CO can be present in the solution (gas stream) [3, 4, 6] or only on the surface [1, 7]. The first case is important for studying the influence of CO adsorption and oxidation on the kinetics of the hydrogen oxidation in PEM fuel cell and for optimising the performance of a reactor for preferential electrochemical CO removal [8]. The second case is of importance in fundamental studies which use the CO oxidation reaction for surface characterisation [1] and in both fundamental and applied studies which use CO oxidation for the determination of the electrochemically active surface area [7, 9].

In the present study the oxidation of CO adsorbed on the surface is investigated. In principle CO adsorbed on the surface can be oxidised in a stripping scan or in a potential step. Both possibilities have been well studied in literature and there is a vast of experimental and theoretical data [1, 2, 7, 9–11]. Here the removal of CO adsorbed on the surface in a stripping scan is investigated. The CO stripping voltammetry is chosen since it is very often used in most experimental studies for the determination of the surface area of PtRu catalysts, e.g. [12]. This method is very promising, but it has many uncertainties (the main one is the CO charge correction in respect to other contributions, like double layer charging and charging due to metal oxide formation, i.e. a baseline subtraction), which were already discussed in literature [13]. In our recent paper [14] different strategies for baseline subtraction were tested and an empirical approach for an "accurate" surface area determination of PtRu catalyst in a membrane electrode assembly was suggested. This method uses only the beginning part of the CO stripping peak, assuming to be free of other faradaic (like oxide formation) and non-faradaic contributions (like double layer charging) and thus enables the accurate surface area determination. In the present paper a model of CO oxidation together with experimental data (oxidation of saturated CO monolayer at different sweep rates in the range from 2 to 100 mV s^{-1} at constant temperature (60 °C) and at different temperatures (room −60 °C)) is presented. The aim is to further validate the empirical approach suggested in [14]. The formulated model is based on the Langmuir–Hinshelwood mechanism [15]. This mechanism assumes two reaction steps:

1. water dissociative adsorption and
2. surface reaction between CO and OH on the surface.

The assumption was made that the water dissociative adsorption is in equilibrium. The rate determining step was assumed to be the surface reaction between CO and OH being adsorbed on the surface. Two different kinetic expressions are formulated assuming that the surface reaction is controlled either by an electrochemical or a chemical reaction step. The CO stripping curve is modelled at different sweep rates and at different temperatures. Then, the optimised curves are deconvoluted to partial contributions. Thereby, by means of the mathematical model the charge due to CO oxidation is calculated and the catalyst surface area is estimated.

2 Experimental

All experiments were performed with a Johnson Matthey carbon-supported PtRu catalyst. The total metal loading was 30 wt% and the Pt:Ru atomic ratio was 1:1. The catalyst was applied to a gold substrate (0.5 cm diameter) in the form of a thin film [16]. A suspension of the catalyst with 30 wt% PtRu was made by mixing 1 ml of water and 3.52 mg of the PtRu/C powder. The solution was agitated in an ultrasonic bath for 60 min, and 10 µl of it were

placed on the gold electrode by a micropipette. The drop was dried in a stream of argon for 2 h at room temperature and then 10 µl of 5% Nafion® solution was placed over the layer of the catalyst and left to dry overnight. This procedure leads to reproducible electrode behaviour.

All experiments were performed in a three compartment glass cell with a gold rotating disk electrode (Radiometer analytical) as working electrode and a Pt-wire as a counter electrode. The metal loading on the electrode surface was 53.9 µg cm^{-2}. The reference electrode was a saturated calomel electrode (SCE), but all electrode potentials in the following text were recalculated with respect to standard hydrogen electrode (SHE). The cell was thermostated by the use of a Julabo thermostat with a precision of ±0.1 °C. The supporting electrolyte was 1 M sulphuric acid (Merck, extra pure) and all solutions were prepared using ultra pure water (Millipore, 18 MΩ cm).

CO was pre-adsorbed on the surface at a constant potential (0.094 V) and at a constant temperature by purging 0.1 vol% CO in Argon through the cell. Before CO adsorption on the surface the electrode was conditioned by potential cycling (60 cycles between 0.05 and 0.8 V starting at the open circuit potential). During CO adsorption the electrode was rotated at 2,500 rpm. By performing the CO adsorption at different adsorption times it was obtained that a saturated CO monolayer is formed after 60 min. Therefore, all measurements in the present communication were performed after saturated CO layer has been formed on the surface. After the CO adsorption the cell was purged with nitrogen (99.9999% purity) for 15 min and then the CO stripping scan was performed. In order to ensure that the CO was completely removed from the surface two more scans were applied.

All electrochemical measurements were carried out with a Zahner impedance measurement unit (IM6e).

X-ray diffraction (XRD) data of the catalyst were obtained on an X'PERT-PRO diffractometer from Panan-alytical GMBH. The scan range was from 10° to 90° with a step size of 0.0084° and a counting time of 19.685 s. The wavelength of X-ray was 1.541874 nm. The measurements were performed at a constant irradiated length of 15.0 mm. As a reference sample the standard reference material (NIST 660a) was used.

3 Results and discussion

3.1 Particle size determination

In order to get some estimation of the maximal surface area, an ex-situ particle size determination was performed by means of X-ray diffraction (XRD) and the average particle size is further used for the XRD surface area determination (Eq. 2). The average particle size was determined from the broadening of the peak at a position close to the Pt (220) peak by using the Scherrer equation:

$$d = \frac{0.89 \cdot \lambda}{(B_{2\theta} - B^{r}_{2\theta}) \cdot \theta_{max}} \quad (1)$$

where d is the average particle size in nm, λ the wavelength of X-ray (0.1541874 nm), θ_{max} the angle at the peak maximum, $B_{2\theta}$ the width (in rad) of the peak at half height and $B^{r}_{2\theta}$ the width (in rad) of the peak at half height for the diffractogram of a standard compound in the similar 2θ range. $B_{2\theta}$ has a value of 4.048° (7.06×10^{-2} rad) and $B^{r}_{2\theta}$ a value of 0.067° (1.17×10^{-3} rad). The average particle size determined from Eq. 1 is 2.4 nm.

Assuming that the particles are spherical, the maximal specific surface area was calculated by using the equation:

$$S_{XRD} = \frac{6 \times 10^{3}}{\rho_{PtRu} \cdot d} \quad (2)$$

where S_{XRD} is the specific surface area in $m^2\ g^{-1}$, ρ_{PtRu} is PtRu density in g cm^{-3} and d is the particle diameter in nm. The PtRu density was calculated as follows:

$$\rho_{PtRu} = \rho_{Pt} \cdot \chi_{Pt} + \rho_{Ru} \cdot \chi_{Ru} \quad (3)$$

where ρ_{Pt} is the platinum density (21.4 g cm^{-3}), ρ_{Ru} is the ruthenium density (12.2 g cm^{-3}) and χ_{Pt} and χ_{Ru} are molar fractions of Pt and Ru in the catalyst without carbon. The latter values are calculated assuming that the Pt:Ru atomic ratio is 1:1 (0.5 and 0.5 for Pt and Ru, respectively). The calculated PtRu density (ρ_{PtRu}) has a value of 16.8 g cm^{-3} and the specific surface area calculated by Eq. 2 is 148.8 $m^2\ g^{-1}$.

Taking into account that 10 µl of 3.52 mg cm^{-3} of 30% PtRu/C were applied onto gold substrate the expected maximal surface area of the catalyst is 15.8 cm^2.

3.2 The mechanism of CO stripping

The CO oxidation reaction on noble metal surfaces is generally accepted to be of Langmuir–Hinshelwood type with the overall mechanism represented by the following steps [15]:

$$\text{Step 0: } CO(g) \rightarrow CO_{ads}$$
$$\text{Step 1: } H_2O \leftrightharpoons OH_{ads} + H^+ + e^-$$
$$\text{Step 2: } CO_{ads} + OH_{ads} \rightarrow COOH_{ads} \rightarrow CO_2 + H^+ + e^-$$

The step 0 in the reaction mechanism is the CO adsorption on the catalyst surface. The kinetics of step 0 is not considered in the model, since the CO was pre-adsorbed on the surface (saturated CO coverage). The step 1 is water dissociative adsorption. The OH adsorbed on the surface formed in step 1 is consumed in step 2 (surface reaction

between CO and OH adsorbed on the surface). The step 2 in the mechanism can be decomposed into two steps and the possibility of $COOH_{ads}$ formation can be considered.

To analyse the CO removal from the surface in the stripping scan a non-linear mathematical model, based on reactions described by step 1 and step 2 above, was developed. The following model assumptions were made:

(i) A mean field approximation was assumed. The assumption is that the CO and OH diffusion rates are much higher than the reaction rate of CO and the OH surface reaction. It is assumed that the reactants are homogeneously distributed on the surface (due to the fast diffusion) and that the reaction rate is proportional to the product of CO and OH average coverage.

(ii) The CO is linearly bonded. Cuesta et al. [17] have shown that on a polycrystalline Pt electrode CO is predominately linearly bonded, while only a small fraction is bridge bonded CO. The ratio between these two species depends on the CO adsorption potential and the quantity of latter species decreases with increasing CO adsorption potential. Similar was obtained in a Lin et al. study [18] where CO oxidation on a Ru-modified Pt(111) electrode was studied. The practical consequence of the assumption above is that one CO molecule blocks one surface site and that upon CO oxidation two surface sites are set free (the other surface site is occupied by adsorbed OH).

(iii) The probability of CO adsorption on both Pt and Ru is the same. This assumption is in accordance to the results of several experimental studies [9, 19, 20]. Bock et al. [20] used the combination of $(COOH)_2$ oxidation and CO stripping to estimate the number of CO molecules which adsorb on PtRu catalysts with different Pt:Ru ratio and they obtained that the probability of CO to adsorb on both Pt and Ru is the same. Wang et al. [9] have shown that for $PtRu_{20}$ catalysts (Pt:Ru atomic ratio is 1:20) the CO saturated coverage is 0.66. This value is between the expected CO monolayer coverage on a Pt(111) surface (0.75) and the CO monolayer coverage on Ru(0001) surface (0.5–0.67). Therefore the value is in the expected range for a mixed PtRu surface.

(iv) Water dissociative adsorption (step 1) is in equilibrium [21].

(v) The water preferential adsorbs at Ru surface sites. The dissociation of water at the Ru sites induces co-adsorption of water at a neighbouring Pt sites. In this way the hydroxyl intermediate can diffuse on the surface. This assumption is in correspondence to the findings of Desai and Neurock [22]. They investigated the interaction of water with a PtRu surface. The initial water dissociation at Ru surface sites leads to the formation of a solvated proton and a surface hydroxyl intermediate centred at the initial Ru adsorption sites. This process induces further co-adsorption of water at a neighbouring Pt sites. The OH intermediate at the Ru sites abstracts a proton from the water which has adsorbed on the Pt-site. As a result the Ru-OH is converted to Ru-H_20, whereas the Pt-water is converted to Pt-OH. In this way the hydroxyl intermediate can diffuse on the surface [22] and can be considered to be homogeneously distributed on the surface. This assumption is valid for well-mixed Pt:Ru surfaces, which corresponds to a kind of catalyst used in the present study (Pt:Ru 1:1). As a result of this assumption, only reaction constants for the water dissociative adsorption on Ru are considered. The rate of OH surface diffusion (from Ru to Pt) was assumed to be fast.

(vi) The anion adsorption and desorption was not taken into consideration. Cuesta et al. [17] have found that the influence of anion adsorption becomes significant at more positive potentials where most of the CO is already stripped from the surface and the competition between anions and OH for the adsorption sites starts to take place [17].

(vii) The surface reaction was assumed to be an irreversible reaction. For the surface reaction two rate constants are assumed. One rate constant corresponds to the oxidation of CO adsorbed on Pt and another to the oxidation of CO adsorbed on Ru. This assumption is in accordance to Fourier Transform Infra Red (FTIR) spectroscopy study of CO adsorbed at PtRu catalyst [23] which showed the presence of different CO IR bands assigned to CO adsorbed on Pt and CO adsorbed on Ru.

Based on the assumptions listed above, balance equations for the surface coverage of the CO and OH adsorbed on the surface are formulated:

$$\frac{d\theta_{OH}}{dE} = \frac{1}{v} \cdot (r_{OH\_1} - r_{OH\_-1} - r_{CO\_Pt} - r_{CO\_Ru}) \tag{4}$$

$$\frac{d\theta_{CO\_Pt}}{dE} = -\frac{1}{v} \cdot r_{CO\_Pt} \tag{5}$$

$$\frac{d\theta_{CO\_Ru}}{dE} = -\frac{1}{v} \cdot r_{CO\_Ru} \tag{6}$$

where v is the sweep rate and r_{OH_1} is the rate of OH adsorbed formation (step 1 in the reaction mechanism, forward reaction). It is given by:

$$r_{OH\_1} = k_1 \cdot (1 - \theta_{OH} - \theta_{CO\_Pt} - \theta_{CO\_Ru}) \cdot \exp\left[\frac{\alpha_1 \cdot \mathrm{F} \cdot E(t)}{\mathrm{R} \cdot T}\right]. \tag{7}$$

By r_{OH_-1} the rate of OH adsorbed desorption (step 1 in the reaction mechanism, backward reaction) is denoted:

$$r_{OH\_-1} = k_{-1} \cdot \theta_{OH} \cdot \exp\left[-\frac{(1-\alpha_1) \cdot F \cdot E(t)}{R \cdot T}\right] \quad (8)$$

r_{CO_Pt} denotes the rate of CO oxidation on platinum:

$$r_{CO\_Pt} = k_{2\_Pt} \cdot \theta_{OH} \cdot \theta_{CO\_Pt} \cdot \exp\left[\frac{\alpha_{2\_Pt} \cdot F \cdot E(t)}{R \cdot T}\right] \quad (9)$$

and r_{CO_Ru} the rate of CO oxidation on ruthenium:

$$r_{CO\_Ru} = k_{2\_Ru} \cdot \theta_{OH} \cdot \theta_{CO\_Ru} \cdot \exp\left[\frac{\alpha_{2\_Ru} \cdot F \cdot E(t)}{R \cdot T}\right] \quad (10)$$

The meaning of the other symbols is as usual, i.e. θ_{OH}, $\theta_{CO\_Pt}, \theta_{CO\_Ru}$ are OH and CO adsorbed on platinum and on ruthenium surface coverages, α_i are the transfer coefficients, F is Faraday's constant, $E(t)$ the electrode potential, R the universal gas constant and T the temperature. The surface coverage θ_{CO_Pt} refers to the total surface, that is $\theta_{CO\_Pt} = x_{Pt} \cdot \theta'_{CO\_Pt}$, where x_{Pt} is the atomic fraction of Pt atoms on the surface,and θ'_{CO_Pt} is the "usual" surface coverage, determined as the ration between the occupied platinum surface sites and the total number of platinum surface sites. Similarly θ_{CO_Ru} is defined. The electrode potential is scanned linearly with time t, at a sweep rate v, starting from initial potential (E_{ini}) (here the initial potential is the CO adsorption potential). The dependence of the electrode potential on time is given by the equation: $E(t) = E_{ini} + v \cdot t$. The unit of the k_i constants (Eqs. 7–10) is s^{-1} since they include the number of H_2O and H^+ molecules (constants k_1 and k_{-1}, respectively) and the total number of the available surface sites (constants k_{2_Pt} and k_{2_Ru}). The number of H_2O and H^+ molecules which are involved in step 1 in the reaction mechanism showed above was assumed to be constant and therefore was included in the reaction constants (k_1 and k_{-1}).

The current due to OH formation and consumption (steps 1 and 2) is determined by using the following equation:

$$I_{OH} = Q_m \cdot \frac{d\theta_{OH}}{dE} \cdot v \quad (11)$$

where Q_m is the charge for the formation of a monolayer of monovalent adsorbed species on the catalyst surface. The Q_m charge is equal to:

$$Q_m = N_{max} \cdot \frac{F}{N_A} \quad (12)$$

where N_{max} is the maximal number of the surface sites, F is the Faraday constant and N_A is the Avogadro constant. The currents for CO oxidation on Pt and Ru are defined by the following equations:

$$I_{CO\_Pt} = n_e \cdot Q_m \cdot r_{CO\_Pt} \quad (13)$$

$$I_{CO\_Ru} = n_e \cdot Q_m \cdot r_{CO\_Ru} \quad (14)$$

where n_e is the number of exchanged electrons.

Besides the faradaic currents the double layer charging current was also added to the total CO stripping current. The double layer charging current was assumed to follow the equation:

$$I_{DL} = v \cdot \left((c_{DL\_Me})_{\theta_{CO}=0} + c_f \cdot (\theta_{CO\_Pt} + \theta_{CO\_Ru})\right) \quad (15)$$

where c_{DL_Me} is the double layer capacitance of the metal surface in absence of CO (the same value was assumed for platinum and ruthenium surface 1.87, 2.16 and 2.56 mF at 22, 40, 60 °C, respectively) and c_f is a constant. It is assumed that the double layer capacitance of the metal surface changes linearly with the CO coverage which is in accordance to [24]. Consequently, the constant c_f can be calculated as:

$$c_f = \frac{(c_{DL\_Me})_{\theta_{CO}=0} - (c_{DL\_Me})_{\theta_{CO}=0.98}}{0 - 0.98} \quad (16)$$

where 0.98 is assumed to be saturated total CO coverage. The values for the double layer capacitance in absence of CO and at saturated CO coverage are determined from the experimental data in the double layer region (app. 0.3 V) and in the "hydrogen adsorption/desorption" region (app. 0.1 V), respectively. The following c_f values have been calculated: −1.41, −1.74 and −2.11 mF at 22, 40 and 60 °C, respectively. The influence of the anion adsorption on double layer capacitance is neglected, while the influence of OH adsorption is taken into account through the contribution of I_{OH} current which should roughly correspond to the pseudo-capacitive current contribution due to surface oxide formation [25].

The total CO oxidation current is the sum of the partial current contributions:

$$I = I_{OH} + I_{CO\_Pt} + I_{CO\_Ru} + I_{DL}. \quad (17)$$

The evaluation of CO charge is done by integration of the surface area under the peak obtained from the contributions of the CO oxidation currents (I_{CO_Pt} and I_{CO_Ru}).

The OH and CO coverages on the surface are obtained by solving the system of balance Eqs. 4–6 (Matlab solver `ode15s` is used). The I_{OH} current is obtained by using Eq. 12 while the CO stripping currents as a function of potential are calculated by using Eqs. 13 and 14. The unknown rate constants are obtained by fitting the calculated curve (Eq. 17) to experimental data. To minimise the deviation between experimental and calculated data the Matlab function `fmin` is used.

In the following the experimental CO stripping results will be discussed. Afterwards the simulation results are presented.

3.3 Analysis of the CO stripping voltammograms

3.3.1 Experimental results

The CO stripping voltammograms of PtRu carbon supported catalyst are collected at different sweep rates (2–100 mV s^{-1}) and at 60 °C. For the sake of clarity only data at one sweep rate (50 mV s^{-1}) are presented (Fig. 1). The shape of the CO stripping peak is in accordance to literature results for similar catalysts [12]. Most of the experimental studies report one peak for CO stripping on the PtRu catalyst [12, 20]. In Fig. 1, besides the main CO stripping peak, another much smaller peak appears at more positive potentials and its position changes with the sweep rate (approximately 0.65 V at 5 mV s^{-1} and 0.7 V at 200 mV s^{-1}). The CO is completely removed in the first cycle and the currents in the second cycle coincide with the PtRu base voltammetry (in absence of CO).

3.3.2 Simulation results

3.3.2.1 Water dissociative adsorption: step 1 The first step in the Langmuir–Hinshelwood mechanism is the water dissociative adsorption. As it was already mentioned this reaction is assumed to be in equilibrium [21]. The next assumption which is made is that Langmuir adsorption conditions are valid for OH adsorption. However, the Langmuir adsorption for OH should yield a well-expressed peak in cyclic voltammogram in absence of CO, which is

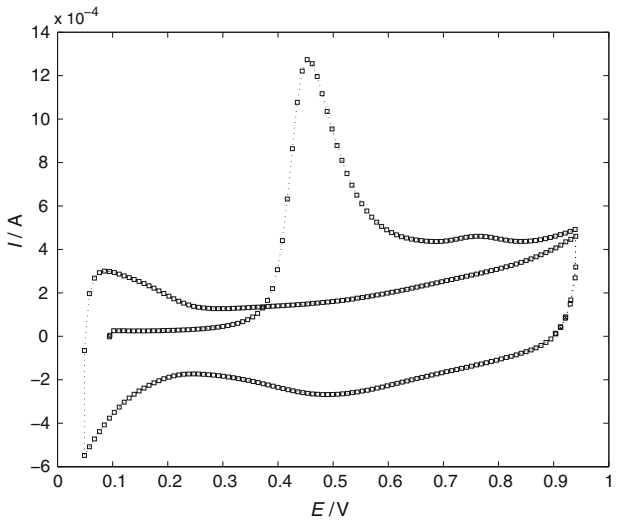

Fig. 1 CO stripping voltammograms of PtRu/C catalyst at 50 mV s^{-1} Conditions: CO adsorption at 0.094 V for 60 min, temperature 333.15 K, 1 M H_2SO_4

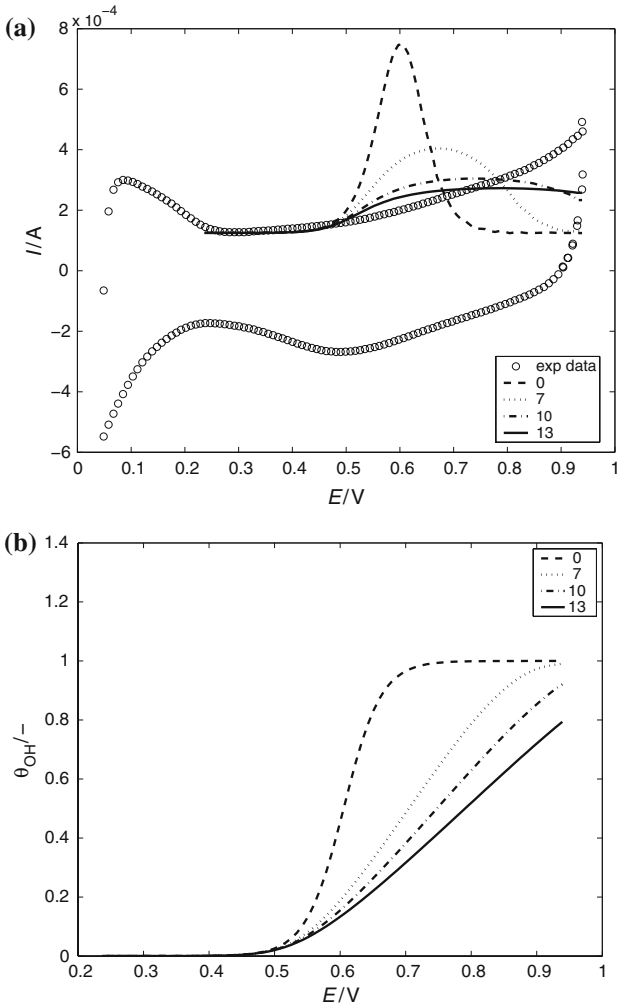

Fig. 2 (**a**) Experimental cyclic voltammogram of PtRu/C catalyst in absence of CO and calculated curves (only anodic direction) assuming different g_{OH} values; (**b**) Calculated OH coverage for different g_{OH} values. Conditions: sweep rate 50 mV s^{-1}, temperature 333.15 K and 1 M H_2SO_4

not observed (Fig. 2a). If the Frumkin/Temkin type of adsorption is assumed the peak which appears in the cyclic voltammogram will be much broader (Fig. 2). The introduction of Frumkin/Temkin adsorption conditions reflects in the reaction constants k_1 and k_{-1}:

$$k_1 = k_{1,0} \cdot \exp[-\beta_{OH} \cdot g_{OH} \cdot \theta_{OH}] \quad (18)$$

and

$$k_{-1} = k_{-1,0} \cdot \exp[(1 - \beta_{OH}) \cdot g_{OH} \cdot \theta_{OH}] \quad (19)$$

where $k_{1,0}$ and $k_{-1,0}$ are intrinsic reaction constants, β_{OH} is a symmetry factor and g_{OH} is a heterogeneity/interaction factor. The simulation results for step 1, i.e. water dissociative adsorption using Frumkin/Temkin isotherm and assuming different values of heterogeneity/interaction factor (g_{OH}) are shown in Fig. 2. The simulated curves (Fig. 2a) are calculated using Eq. 17 and by setting I_{CO_Pt}

Table 1 Results of the validation of the models

	Variety 1: chemical r.d.s.	Variety 2: electrochemical r.d.s.	Variety 1: chemical r.d.s. (data ref. [7])
$k_{1,0}/s^{-1}$	4.00×10^{-4}	4.00×10^{-4}	4.00×10^{-4}
$k_{-1,0}/s^{-1}$	5.43×10^{5}	5.43×10^{5}	5.43×10^{5}
$k_{2,0\_Pt}/s^{-1}$	8.11	6.00×10^{-4}	8.11
$k_{2,0\_Pt}/s^{-1}$	22.11	6.11×10^{-3}	22.11
α_1	0.5	0.5	0.5
α_{2_Pt}	0	0.5	0
α_{2_Ru}	0	0.5	0
g_{OH}	13	13	13
g_{CO_Pt}	5	8	5
g_{CO_Ru}	10	10	10
$\Delta H_{ads}/kJ\ mol^{-1}$	70.0	–	70.0
$E_{a,Pt}/kJ\ mol^{-1}$	20.0	–	20.0
$E_{a,Ru}/kJ\ mol^{-1}$	40.0	–	40.0
N_{max}	9.5×10^{15}	8.5×10^{15}	6.5×10^{15}
θ_{CO_Pt}	0.49	0.49	0.49
θ_{CO_Ru}	0.49	0.49	0.49

and I_{CO_Ru} to zero (CO coverage on the surface is zero). The OH coverages in Fig. 2b are calculated using Eq. 4 (again due to zero CO coverage, the reaction rates r_{CO_Pt} and r_{CO_Ru} are equal to zero). The heterogeneity/interaction factor 0 corresponds to Langmuir adsorption conditions. The symmetry factor (β_{OH}) in the Frumkin/Temkin isotherm is assumed to be 0.5. The values of the $k_{1,0}$ and $k_{-1,0}$ constants and of the transfer coefficient α_1 are summarised in Table 1. Further simulations are performed using heterogeneity/interaction factor 13, since it gives the best approximation of the real conditions.

3.3.2.2 Surface reaction: step 2 CO adsorption conditions: The step 2 is the surface reaction between CO and OH adsorbed on the surface. As it was mentioned before this step can be controlled by a chemical reaction (formation of COOHads) or an electrochemical reaction (formation of CO_2). This makes two model varieties, but before discussing them in details, CO adsorption conditions on the surface will be discussed. Similar to the OH adsorption, the change of the CO adsorption conditions will influence the k_{2_Pt} and k_{2_Ru} reaction constants:

$$k_{2\_Pt} = k_{2,0\_Pt} \cdot \exp\left[\beta_{CO\_Pt} \cdot g_{CO\_Pt} \cdot \theta_{CO\_Pt} + \beta_{OH} \cdot g_{OH} \cdot \theta_{OH}\right] \quad (20)$$

$$k_{2\_Ru} = k_{2,0\_Ru} \cdot \exp\left[\beta_{CO\_Ru} \cdot g_{CO\_Ru} \cdot \theta_{CO\_Ru} + \beta_{OH} \cdot g_{OH} \cdot \theta_{OH}\right] \quad (21)$$

The Langmuir adsorption conditions correspond to heterogeneity/interaction factors (g_{CO_Pt}, g_{CO_Ru}) zero which result in a very sharp CO stripping peak. In Fig. 3a, b the simulation results for $g_{CO\_Ru} = 0$ (Langmuir adsorption conditions) and different values of g_{COPt} (1–10) are shown. The α_{2_Pt} and α_{2_Ru} values are set to zero, since it was assumed that the surface reaction is dominated by the chemical reaction. The water dissociative adsorption is described using the conditions mentioned in Fig. 2 ($g_{OH} = 13$). The simulated curves in Fig. 3a are calculated using Eq. 17. As starting CO coverages, $\theta_{CO\_Pt} = \theta_{CO\_Ru} = 0.49$ are assumed, that the total initial CO coverage is 0.98 and $x_{Pt} = x_{Ru} = 0.5$. By increasing of g_{CO_Pt} (Frumkin/Temkin adsorption isotherm) the CO stripping peak is becoming broader and it moves to a more negative potential region. This is due to the additional term of the form $\exp[\beta_{CO\_Pt} \cdot g_{CO\_Pt} \cdot \theta_{CO\_Pt} + \beta_{OH} \cdot g_{OH} \cdot \theta_{OH}]$ in the expression for the rate constant k_{CO_Pt} (Eq. 20), which increases the value of this rate constant and through θ_{CO_Pt} and θ_{OH} introduce an additional dependence on the potential. If the difference between the two rate constants for CO oxidation on Pt and Ru is large enough, one CO stripping peak will split into two separate peaks. This can be seen in Fig. 3a for interaction/heterogeneity factor 10, where a well expressed shoulder appears. The increase of g_{CO_Pt} moves the onset of CO oxidation reaction to a more negative potential region.

Two model varieties: The first model variety assumes that the surface reaction is controlled by a chemical reaction. This means that the surface reaction is independent on the potential and formally the transfer coefficients α_{2_Pt} and α_{2_Ru} for the surface reaction on Pt and Ru (Eqs. 9 and 10) can be set to zero. The second model variety assumes that the surface reaction is an electrochemical reaction, so here the transfer coefficients α_{2_Pt} and α_{2_Ru} are different

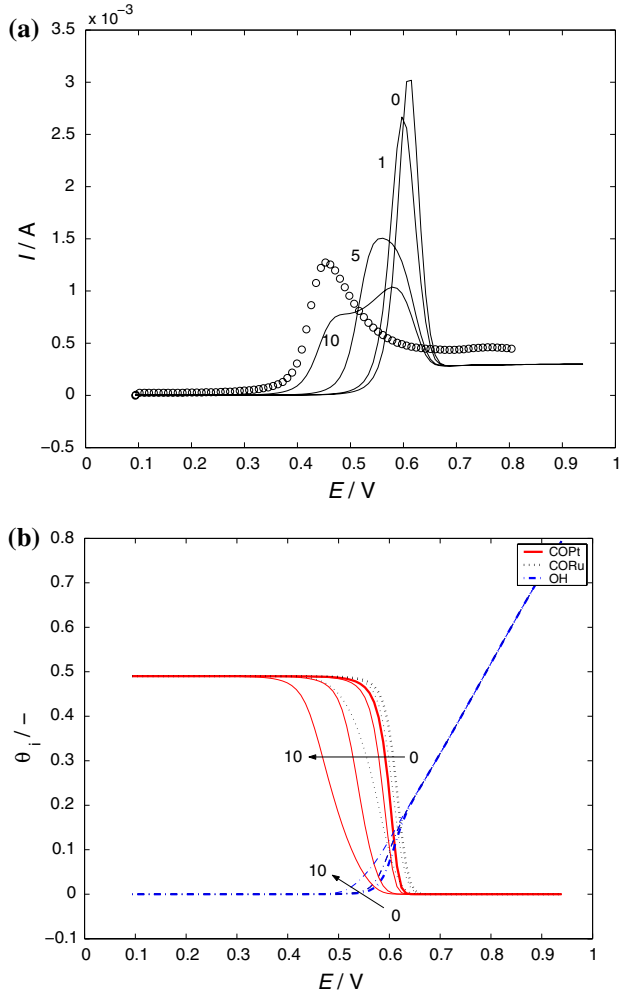

Fig. 3 (**a**) Experimental CO stripping voltammogram of PtRu/C catalyst and calculated curves assuming different g_{CO_Pt} values and constant $g_{CO\_Ru} = 0$ and $g_{OH} = 13$ values; (**b**) Calculated θ_{OH}, θ_{CO_Pt}, θ_{CO_Ru} coverages for different g_{CO_Pt} values. Conditions: sweep rate 50 mV s^{-1}, temperature 333.15 K and 1 M H_2SO_4

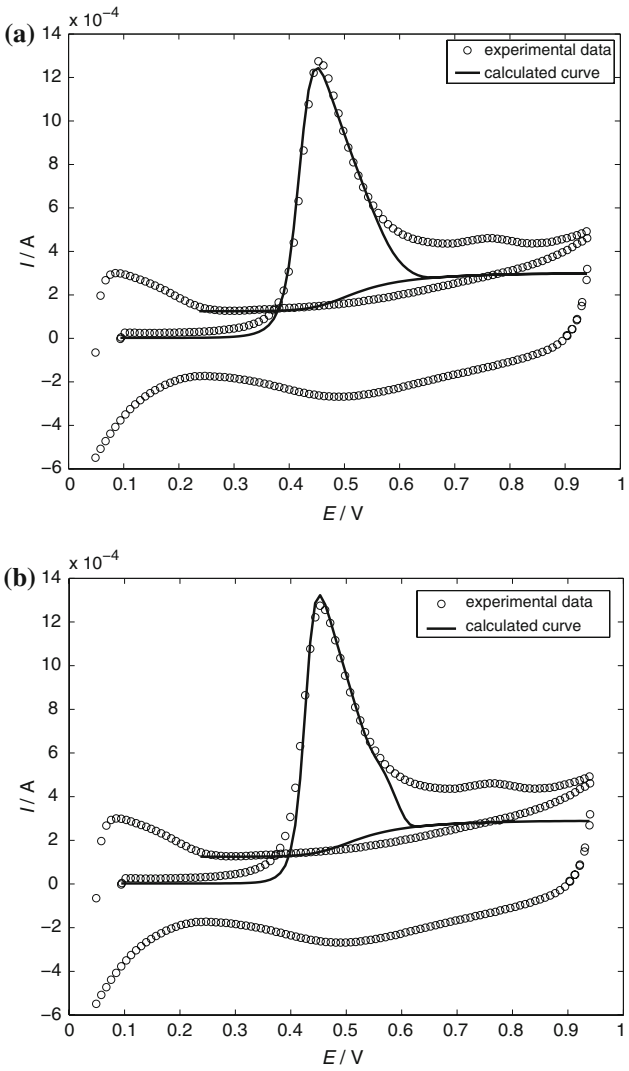

Fig. 4 Experimental CO stripping cyclic voltammogram (first and second scan) and simulated curves (only anodic direction first and second scan) for (**a**) model variety 1 and (**b**) model variety 2. Conditions: CO adsorption at 0.094 V for 60 min, sweep rate 50 mV s^{-1}, temperature 333.15 K and 1 M H_2SO_4. Kinetic parameters from Table 1 (Model varieties 1 and 2)

from zero. The experimental data and the calculated curves for the two model varieties are shown in Fig. 4a, b. In both model varieties the parameter values for the water dissociative adsorption are kept constant and they correspond to the conditions described in Fig. 2. The double layer capacitance and the c_f value (Eq. 16) are also kept constant. The transfer coefficients for step 1 and step 2 (surface reaction electrochemical reaction) are assumed to be 0.5. Also, all symmetry coefficients are assumed to be 0.5. Other values are fitted such that the simulated curve gives the smallest deviation of the experimental data. The parameter values for two different models are summarised in Table 1. As it can be seen in Table 1 the most pronounced difference between two model varieties is reflected in values of two reaction constants (k_{2_Pt} and k_{2_Ru}). If the surface reaction is controlled by the electrochemical step the values of these rate constants are approximately four orders of magnitude less than in the case of the controlling chemical reaction step. This is understandable taking into account the additional exponential term which appears in the case of the electrochemical reaction. The values of other parameters are very similar (there is only a small difference in the value for heterogeneity factor for CO adsorbed on Pt (5 (chemical) vs. 8 (electrochemical)) and for the maximal number of surface sites (9.5×10^{15} vs. 8.5×10^{15} in the case of chemical vs. electrochemical variety) but they are not very significant. In general both model varieties give a reasonable fit to the experimental data. Both model varieties show a deviation in the more positive potential region. Our simulation results predict that in the more positive

potential region the base curve (in absence of CO) coincides with the CO stripping curve. Unlike the model in the experiment an additional charge appears in this potential region. Presently, it is not clear if this charge is a CO stripping charge or if it is due to some other processes. A possible reason for this deviation can be the very simplified description of the water dissociative reaction (surface oxide formation) which is known to be a more complex reaction and includes a higher oxide formation [25]. Another possibility for this deviation can be the neglection of the anion adsorption in our model, which can take place in the more positive potential region. This assumption is additionally supported by experimental results of Yajima et al. [23] who studied CO stripping in base electrolyte with a low anion adsorption ($HClO_4$, unlike H_2SO_4 in our study). In their study the base curve coincides with the CO stripping curve in the more positive potential region, which is in accordance to our simulation results.

Based on the discussion presented above it is not possible to differentiate between two model varieties. The similar conclusion was reached by Desai and Neurock [22]. They calculated the reaction energies for the CO + OH surface reaction for both chemical and electrochemical paths. It was obtained that the difference in the overall reaction energy is insignificant and they concluded that it is difficult to distinguish which of these paths would prevail under electrocatalytic conditions. However the first model variety (chemical reaction) is preferred in the following simulations in accordance to our previous studies where the discrimination between different model varieties in the case of methanol oxidation was performed using electrochemical impedance spectroscopy (EIS) [26].

The influence of sweep rate: The influence of the sweep rate was studied in the sweep rate range between 2 and 100 mV s^{-1}, since this sweep rates were typically used in experimental studies for CO stripping surface area determination. In Fig. 5a, b the simulated (Model variety 1) and experimental data at different sweep rates are shown. The parameter values are given in Table 1 (Model variety 1). As it can be seen, the agreement between experimental and simulated curves at both low and the high sweep rate is reasonable. The model can predict the sweep rate dependence of the onset, the peak potential, the height of the peak, as well as the peak broadness. As it was discussed before, the model shows a deviation at a more positive potential values, but this point was already discussed above. The height of the peak shows a small deviation at a sweep rate of 10 mV s^{-1}. This deviation can occur due to a small difference in the real catalyst surface area between different experiments. In the model this mostly reflects in N_{max} (maximal number of surface sites). The influence of the variation of N_{max} on simulated curves, at the sweep rate of 10 mV s^{-1} was checked (not shown here). It can be seen

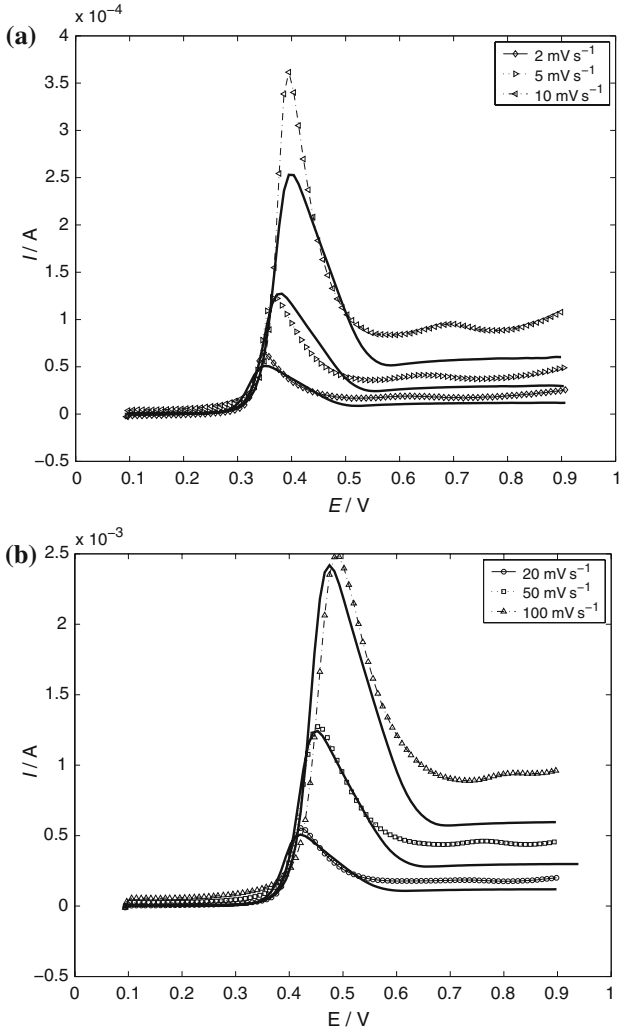

Fig. 5 Experimental (concatenated symbols) and calculated—Model variety 1 (full lines) CO stripping voltammograms of PtRu/C catalyst at different sweep rates. (**a**) 2, 5, 10 mV s^{-1} and (**b**) 20, 50, 100 mV s^{-1}. Conditions: CO adsorption at 0.094 V for 60 min, temperature 333.15 K, 1 M H_2SO_4. Kinetic parameters from Table 1 (Model variety 1)

that the peak height is mainly controlled by N_{max}. Another parameter which can influence the peak height at constant N_{max} is the CO surface coverage (see Fig. 6b).

The influence of temperature: The CO stripping experiments are performed at different temperatures in the temperature range from 22 (room) to 60 °C and at the sweep rate of 50 mV s^{-1}. The experimental results are shown in Fig. 6a. The increase of the temperature causes a shift of the CO stripping curve to a lower potential region. The shape of the CO stripping peak is basically unchanged (peak broadness), but the peak height shows some small variations. The cyclic voltammograms in absence of CO show the difference in the double layer region (app. 0.25–0.3 V) and the double layer capacitance increases slightly with the temperature (1.87 mF at 22 °C and 2.56 mF at

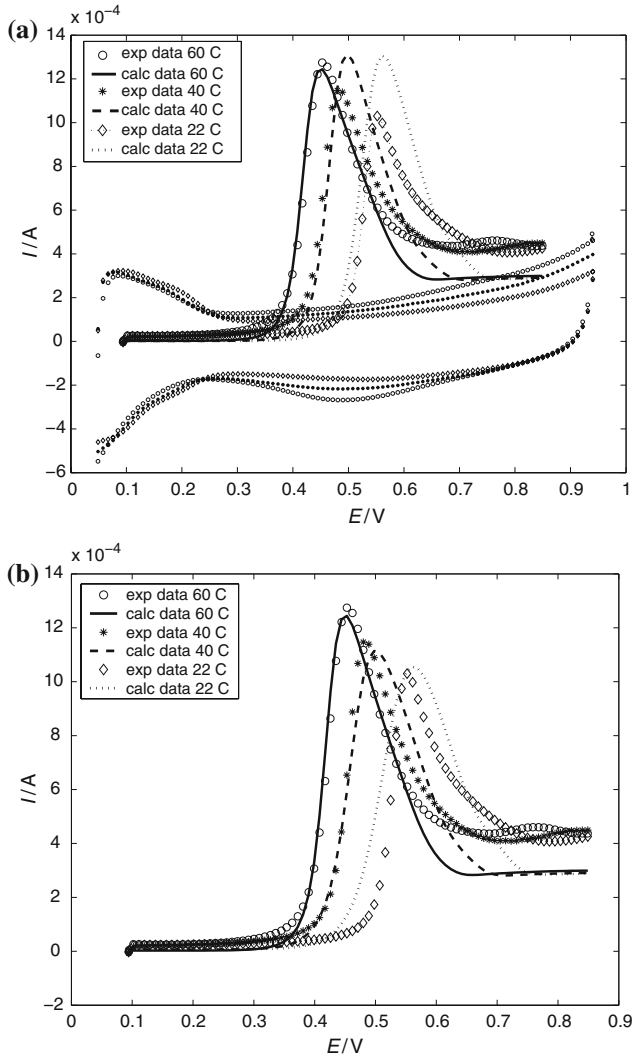

Fig. 6 Experimental and simulated CO stripping voltammograms at different temperatures. (**a**) Kinetic parameters from Table 1 (Model variety 1). (**b**) The values of CO coverage is adjusted to fit better the curves at lower temperatures. Other kinetic parameters same as in (**a**). Conditions: CO adsorption at 0.094 V for 60 min, sweep rate 50 mV s^{-1}, 1 M H_2SO_4

60 °C). The difference can be also seen in the more positive potential region which is related to the temperature influence on the surface oxide formation. For the model description of the experimental data it is assumed that the rate constants are temperature dependent:

$$\left(\frac{k_{1,0}}{k_{-1,0}}\right)_T = \left(\frac{k_{1,0}}{k_{-1,0}}\right)_{T=60^\circ\mathrm{C}} \cdot \exp\left[-\frac{\Delta H_{\mathrm{ads}}}{\mathrm{R}}\left(\frac{1}{T}-\frac{1}{273.15+60.0}\right)\right] \quad (22)$$

$$\left(k_{2,0\_i}\right)_T = \left(k_{2,0\_i}\right)_{T=60^\circ\mathrm{C}} \cdot \exp\left[-\frac{E_{a,i}}{\mathrm{R}}\left(\frac{1}{T}-\frac{1}{273.15+60.0}\right)\right] \quad (23)$$

where, ΔH_{ads} is the enthalpy of adsorption for the water dissociative adsorption step, $E_{a,i}$ are the activation energies for the surface reaction and i denotes Pt or Ru. The enthalpy of the adsorption and activation energies are used as additional fitting parameters to fit the experimental CO stripping curves at different temperatures and their values are given in Table 1 (only for model variety 1). For these simulations it is assumed that the heterogeneity/interaction factors, transfer and symmetry coefficients are temperature independent, since the temperature interval is not very large. The enthalpy of adsorption for the water dissociative adsorption has a value of 70.0 kJ mol^{-1}. This value has been chosen in order to give a similar shift of the onset potential of OH adsorption as seen in the cyclic voltammograms in absence of CO (Fig. 6a). The activation energies for the surface reaction on Pt and Ru are 20 and 40 kJ mol^{-1}, respectively. As can be seen in Fig. 6a the simulated curves show a good agreement to the experimental data. In the more positive potential region the simulated curves show a deviation in comparison to the experimental data (as it was already discussed), but the tendency predicted by the model is correct. The model predicts a small increase of the peak current with a decrease of temperature, while the experimental curves show an opposite tendency. It was already discussed that the variations in the peak current can be due to small variations in the real surface area which can slightly vary from experiment to experiment (the precision of thin film method [16]) or to some small difference in the CO surface coverage. The second possibility is checked in Fig. 6b, where the curves at room temperature and 40.0 °C are simulated for a total CO coverage (0.94 and 0.96, respectively) and a better agreement to experimental data was obtained.

3.4 The CO stripping peak deconvolution

As it was mentioned in the introduction we intend to use the calculated CO stripping curve to perform the CO stripping peak deconvolution and to separate the CO stripping charge from other contributions which makes the voltammetric CO charge determination less accurate [13]. The CO stripping peak deconvolution is demonstrated in Fig. 7 for the sweep rate of 50 mV s^{-1}. The simulated curve is calculated by using the model variety 1. The grey lines (full and dotted line) correspond to the CO currents and they were used to calculate the CO charge. The calculated CO charges at different sweep rates are summarised in Table 2. Taking the CO charge values, the total CO coverage (0.98) and assuming 420 μC cm^{-2} as an elementary charge for a 2 electron process the real surface area values are determined (Table 2). The mean value of

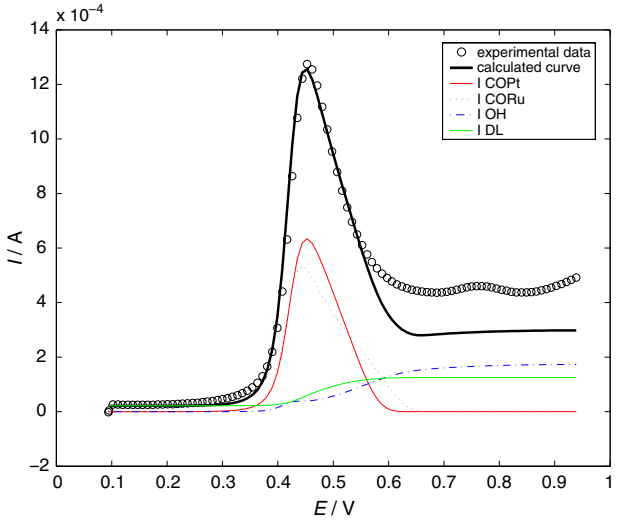

Fig. 7 The CO stripping peak deconvolution. Conditions: sweep rate 50 mV s^{-1}, temperature 333.15 K and 1 M H_2SO_4. Kinetic parameters from Table 1 (Model variety 1)

Table 2 Model calculated (Variety 1) relative error, percent of CO charge consumed up to half peak potential and surface area

Sweep rate/mV s^{-1}	ε_{rel}/%	ε_{CO}/%	S/cm^2
2	2.04	8.45	6.78
5	2.37	9.7	6.72
10	2.73	8.87	6.72
20	3.48	8.92	6.73
50	5.53	8.89	6.72
100	8.60	8.78	6.74

the surface area calculated at different sweep rates is 6.73 ± 0.03 cm^2. The calculated value is only 42% of XRD surface area (6.73 cm^2 in comparison to 15.8 cm^2). This result is in agreement to results of other literature studies, which showed a deviation between, e.g. BET and CO stripping area (e.g. in [7] CO stripping area is approx 45–52% of BET surface area).

3.5 Comparison with an empirical method and literature data

As it was mentioned above,the practical problem in voltammetric CO charge determination using experimental data is a baseline subtraction. In praxis, it is usually assumed that baseline is the same as in absence of CO, or that it can be approximated by a straight line. Both options can lead to significant deviations between the calculated and the real surface area [7, 14]. In our previous paper an empirical method for "accurate" voltammetric CO charge determination is proposed [14]. This method assumes that the CO charge at the onset of the CO stripping curve is not influenced by other faradaic and non-faradaic contributions. If the CO stripping curve is integrated only up to the half peak potential (assuming that the base line is a linear extension of the CO stripping line), and enlarged approximately for a factor 10 (this was determined in an independent experiment with platinum) the determined charge is independent on the sweep rate. So the main assumptions of our empirical method are:

1. the base line in the potential region up to the half peak potential can be approximated by a straight line, which is the extension of the CO stripping line, and
2. the CO charge consumed up to the half peak potential is proportional to the total CO stripping charge, and the proportionality factor is independent of the sweep rate.

These two assumptions can be now validated by the proposed mathematical model. In Fig. 8a, b the simulated curves at sweep rates 2 (Fig. 8a) and 100 mV s^{-1} (Fig. 8b) are presented. The baselines in absence of CO (dotted line) and in presence of CO (dashed line) are also shown. The hatched areas in Fig. 8a, b correspond to the CO charge consumed up to the half peak potential. According to the simulated results the baseline in presence of CO (dashed line) in the potential region up to the half peak potential (hatched area) deviates from linearity at both sweep rates, but the deviation is stronger expressed at higher sweep rates (100 mV s^{-1}). If the baseline is approximated by the straight line (assumption "a") the percent error can be calculated as:

$$\varepsilon_{rel} = \frac{(\theta_{CO,I=I_{p/2}})_{approx} - (\theta_{CO,I=I_{p/2}})_{exact}}{(\theta_{CO,I=I_{p/2}})_{exact}} \cdot 100 \qquad (24)$$

where $\theta_{CO,I=I_{p/2}}$ is the CO stripping charge consumed up to the half peak potential and the indices *approx* and *exact* denote the approximated (straight line) and the real (model calculated) baseline. In the sweep range 2–100 mV s^{-1} the error ε_{rel} (24) is in the range between 2.04 and 8.78% (the values for different sweep rates are summarised in Table 2). This would mean that for the voltammetric CO charge determination the experimental data at lower sweep rates are more suitable. The ratio of CO charge consumed up to the half peak potential with respect to the total CO charge can be calculated as follows:

$$\varepsilon_{CO} = \frac{\theta_{CO,I=I_{p/2}}}{\theta_{CO,total}} \cdot 100 \qquad (25)$$

The ε_{CO} values at the different sweep rates are presented in Table 2. The mean value is 8.93 ± 0.41%. According to the model predictions the approximation of the baseline as a straight line can be used with a higher certainty at low sweep rates and the ratio of the CO charge consumed up to the half peak potential is constant at different sweep rates.

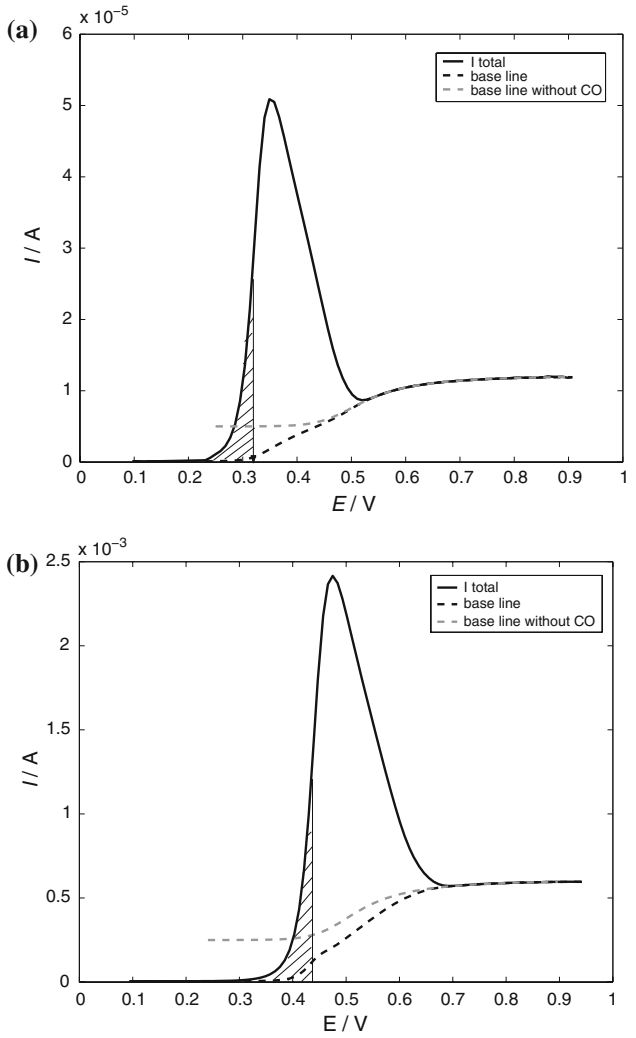

Fig. 8 The influence of sweep rate on the baseline deviation from the linearity in the potential region up to the half peak potential. Simulation results at (**a**) 2 and (**b**) 100 mV s^{-1}. Kinetic parameters from Table 1 (Model variety 1)

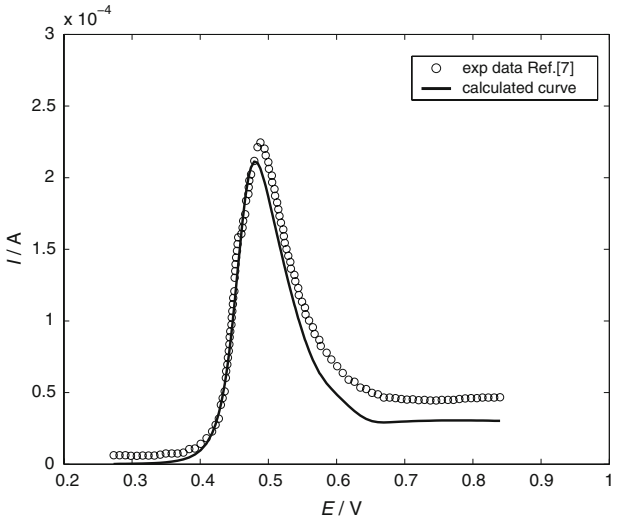

Fig. 9 The experimental (data from ref. 7]) and the simulated CO stripping voltammograms. Conditions: sweep rate 10 mV s^{-1}, temperature 293.15 K. Kinetic parameters from Table 1 (Model variety 1-Data [7])

It can be concluded that the assumptions of the empirical model are reasonable (especially at low sweep rates) and it can be used for reliable experimental CO voltammetric charge determination.

Finally, our method is compared to literature data [7]. These data are chosen since the CO charge in [7] was determined by using the differential electrochemical mass spectrometry (DEMS), which should give a better estimation of CO charge. In Fig. 9 the experimental data from reference [7] and the simulated curves using model variety 1 are shown. The model parameters are summarised in Table 1 and as can be seen they correspond to the parameter values determined from experimental data in the present study. The difference is only in N_{max}. The N_{max} value is determined from the known real CO charge value for this catalyst (1.9 mC, DEMS data). As can be seen in Fig. 9 a very good agreement to experimental data is obtained. The deviation is observed only in the more positive potential region, which can be due to anion adsorption neglection as it was already discussed above.

4 Conclusions

The determination of the real surface area under working conditions (fuel cell conditions) has a great practical relevance in the fuel cell community (evaluation of the catalyst deuteration under working conditions). The most common solution in daily fuel cell praxis is a surface area determination by use of CO stripping. The method however is not accurate from the reasons discussed above. In this study a mathematical model of CO stripping voltammetry based on the Langmuir–Hinshelwood mechanism was developed. The model can predict the sweep rate dependence of the onset of CO oxidation, the peak potential, peak current and peak broadness. The small deviations between the model and the experimental data are observed in the more positive potential region. These deviations can be due to neglection of anion adsorption in the model. The model proposed here enables the CO stripping peak deconvolution and the separation of the CO stripping charge from other faradaic and non-faradaic contributions, which is the main difficulty in the voltammetric CO charge determination. The model predicts baseline deviation from linearity, in the potential region up to the half peak potential, at all sweep rates. The deviation is the smallest at 2 mV s^{-1} (2.04%) in comparison to 8.78% at 100 mV s^{-1}, so the use of low sweep rates for CO voltammetric charge determination from the

experimental data is suggested. According to the model, approximately 8.93% of the total CO charge is consumed up to the half peak potential and this value is not changing with the sweep rate. The above model predictions validate the use of the empirical method proposed in [14] as a practical approach for the CO stripping charge determination. The real CO stripping charge can be determined by some non-electrochemical methods. An example is DEMS. The experimental results from the literature DEMS study [7] are used for further model validation and a very good agreement is obtained.

Acknowledgments We would like to acknowledge Dr. Heike Lorenz, (Max Planck Institute for Dynamics of Complex Technical Systems in Magdeburg) for performing X-ray catalyst analysis and Mr. Christian Fuchs (Max Planck Institute for Dynamics of Complex Technical Systems in Magdeburg) for making CO stripping measurements.

References

1. Gasteiger H, Marković N, Ross P, Cairns E (1994) J Phys Chem 98:617
2. Koper M, Jansen A, Santen R, Lukkien J, Hilbers P (1998) J Chem Phys B 109:6051
3. Camara G, Ticianelli E, Mukerjee S, Lee S, McBreen J (2002) J Electrochem Soc 149(6):A748
4. Behm R, Jusys Z (2006) J Power Sources 154:327
5. Vidaković T, Christov M, Sundmacher K (2005) J Electroanal Chem 580:105
6. Enback S, Lindbergh G (2005) J Electrochem Soc 151(1):A23
7. Jusys Z, Schmidt T, Dubau L, Lasch K, Jorissen L, Garche J, Behm R (2002) J Power Sources 105:297
8. Zhang J, Datta R (2005) J Electrochem Soc 152(6):A1180
9. Wang J, Branković R, Zhu Y, Hanson J, Adzić R (2003) J Electrochem Soc 150(8):A1108
10. Maillard F, Eikerling M, Cherstiouk O, Schreier S, Savinova E, Stimming U (2004) Faraday Discuss 125:357
11. Koper M, Lebedeva N, Hermse G (2002) Faraday Discuss 121:301
12. Dihn H, Ren X, Garzon F, Zelenay P, Gottesfeld S (2000) J Electroanal Chem 491:222
13. Nart F, Vielstich W (2003) Handbook of fuel cells—fundamentals, technology and applications, vol 2. Wiley, Chichester
14. Vidaković T, Christov M, Sundmacher K (2007) Electrochim Acta 52:5606
15. Gilman S (1964) J Phys Chem 68:70
16. Schmidt TJ, Gasteiger HA, Behm RJ (1999) Electrochem Commun 1:1
17. Cuesta A, Couto A, Rincon A, Perez M, Lopez-Cudero A, Gutierrez C (2006) J Electroanal Chem 586:184
18. Lin WF, Zei MS, Eiswirth M, Ertl G, Iwasita T, Vielstich W (1999) J Phys Chem B 103:6968
19. Gasteiger H, Marković N, Ross P, Cairns E (1994) Electrochim Acta 39:1825
20. Bock C, MacDougall B, LePage Y (2004) J Electrochem Soc 151(8):A1269
21. Saravanan C, Marković N, Head-Gordon M, Ross PN (2001) J Chem Phys 114:6403
22. Desai S, Neurock M (2003) Electrochim Acta 48:3759
23. Yajima T, Uchida H, Watanabe M (2004) J Phys Chem B 108:2654
24. Bilmes SA, Arvia AJ (1986) J Electroanal Chem 198:137
25. Trasatti S, O'Grady W (1981) Advances in electrochemistry and electrochemical engineering, vol 12. Wiley, New York
26. Krewer U, Christov M, Vidaković T, Sundmacher K (2006) J Electroanal Chem 589:148